Food & Function

Impact of pesticide polarity and lipid phase dimensions on the bioaccessibility of pesticides in agricultural produce consumed with model fatty foods

Journal:	*Food & Function*
Manuscript ID	FO-ART-12-2019-003055.R2
Article Type:	Paper
Date Submitted by the Author:	02-Jun-2020
Complete List of Authors:	Zhang, Ruojie; University of Massachusetts, Department of Food Science Zhang, Zipei; University of Massachusetts Amherst, Food Science Li, Ruyi; State Key Laboratory of Food Science and Technology, Tan, Yunbing; University of Massachusetts, Food Science Lv, Shanshan; Northeast Forestry University, College of Material Science and Engineering McClements, David; University of Massachusetts, Food Science

Impact of pesticide polarity and lipid phase dimensions on the bioaccessibility of pesticides in agricultural produce consumed with model fatty foods

Ruojie Zhang [a,1], Zipei Zhang [a, 1], Ruyi Li [a, b], Yunbing Tan [a], Shanshan Lv [a,c], and David Julian McClements [a, d*]

[a]Department of Food Science, University of Massachusetts Amherst, Amherst, MA 01003, USA

[b]Key Laboratory of Food Science and Technology, School of Food, Nanchang University, Nanchang, Jiangxi 330047, China

[c]College of Forestry, Northeast A&F University, Yangling, Shanxi, 712100, China

[d]Laboratory for Environmental Health NanoScience, Center for Nanotechnology and Nanotoxicology, T. H. Chan School of Public Health, Harvard University, 665 Huntington Avenue, Boston, MA 02115, USA

Journal: Food and Function

Submitted: December 2019

[1] These authors contributed equally to this manuscript.

[*]Corresponding author. Department of Food Science, University of Massachusetts, Amherst, MA 01003, USA.

Abstract

For most people, the pesticide residues found on agriculture products are the main source of pesticide exposure, which may adversely influence consumer health. The potential health hazard of residual pesticides depends on the nature of the foods they are consumed with. Studies with fat-soluble vitamins and nutraceuticals have shown that their bioaccessibility depends on food matrix composition and structure. We used an *in vitro* method to investigate the influence of the dimensions of the lipid phase in model fatty foods (emulsified or bulk oil) on the bioaccessibility of various pesticides. Three pesticides that differed in their oil-water partition coefficients were selected: bendiocarb (Log P = 1.7), parathion (Log P = 3.8), and chlorpyrifos (Log P = 5.3). These pesticides were mixed with tomato puree to represent pesticide-treated agricultural products. Three model foods with different oil phase dimensions were used to represent different kinds of food product: small emulsions (d_{32} = 0.14 μm); large emulsions (d_{32} = 10 μm); and, bulk oil. Our results showed that the oil droplets underwent extensive changes as they passed through the simulated gastrointestinal tract due to changes in environmental conditions, such as pH, ionic strength, bile salts, and enzyme activities. The initial rate and final amount of lipid hydrolysis decreased with increasing lipid phase dimensions. Pesticide bioaccessibility depended on both the hydrophobicity of the pesticide and the dimensions of the co-ingested lipid droplets. The least hydrophobic pesticide (bendiocarb) had a high bioaccessibility (> 95%) that did not depend on lipid phase dimensions. The more hydrophobic pesticides (parathion and chlorpyrifos) has a lower bioaccessibility that increased with decreasing lipid phase dimensions. Our results demonstrate the critical role that food structure plays on the potential uptake of pesticides from agricultural products, like fruits and vegetables.

Keywords: emulsions; droplet size; pesticides; hydrophobicity; bioaccessibility;

1. Introduction

Pesticides are widely used as an effective approach to increase agricultural yields by decreasing crop diseases and pest infestations [1, 2]. In the past few decades, however, there has been concern that the presence of pesticide residues on agriculture products may be hazardous to human health [3, 4]. A number of chronic diseases, including Parkinson's disease, neurodegenerative diseases, obesity, and some types of cancer, are linked to pesticide exposure [5-11]. The most common source of pesticide exposure in the general population is from the residues present on agricultural products, like fruits and vegetables. The potential toxicity of pesticides depends on the type and amount present on foods, as well as on the amount of the ingested pesticide that actually gets absorbed by the body[12, 13]. Like other bioactive substances, the bioavailability of pesticides depends on the composition and structure of any foods they are consumed with[14, 15]. In a typical Western diet, agriculture products are commonly consumed with emulsion-based food products, *e.g.,* raw vegetables with dips or dressings, fresh fruits with creams or yogurts, and cooked vegetables with sauces[16]. Consequently, there is interest in how the properties of food emulsions may impact the bioavailability of pesticides.

Emulsions are often consumed with agricultural products to enhance their palatability by altering their appearance, texture, mouthfeel, or flavor. In addition, they have been shown to enhance the bioaccessibility of non-polar nutraceuticals (such as carotenoids) within fruits and vegetables, which may have health benefits [16-18]. Conversely, this food combination may adversely increase the bioavailability, and therefore potential toxicity, of any pesticide residues on the agricultural products. Previously, we studied the impact of several emulsion properties on pesticide bioaccessibility from agricultural produce [14, 15]. We found that pesticide bioaccessibility could be significantly increased by the presence of digestible fat particles in co-ingested emulsions. The molecular structure of the lipid phase also played an important role

in pesticide bioaccessibility because it influenced the ability of mixed micelles present in the small intestinal fluids to solubilize the pesticides. In particular, a significantly higher pesticide bioaccessibility was observed in the presence of fat droplets comprised of long-chain fatty acids than in those comprised of median chain fatty acids. Here, we focus on the impact of the dimensions of the lipid phase in fatty foods on the bioaccessibility of several hydrophobic pesticides, since the fatty domains within foods may vary considerably.

The pesticides used to treat agricultural crops vary considerably in their molecular characteristics, particularly their sizes and polarities. We hypothesized that these molecular features would influence pesticide bioaccessibility by altering their ability to be solubilized by the gastrointestinal fluids formed after the samples were digested. In the current research, we therefore selected three pesticides with different molecular properties: bendiocarb, parathion, and chlorpyrifos. Model foods with different oil droplet sizes were used in this study to represent different kinds of emulsified food products that may be consumed with fruits and vegetables. These products may vary widely in their droplet sizes, which could impact their rate and extent of lipid digestibility, and therefore impact pesticide bioaccessibility. For instance, salad dressings and mayonnaises typically contain relatively large oil droplets (2 to 20 μm), whereas milks and creams contain much smaller ones (0.2 to 2 μm).

The insights obtained from this study should facilitate the prediction of the impact of co-consumed food products on the uptake and toxicity of pesticide residues found in agricultural produce.

2. Materials and methods

2.1 Materials

Fresh tomatoes (organic) and corn oil (Mazola, ACH Food Companies, Inc.) were bought from a local supermarket. Pesticide standards (bendiocarb, parathion, chlorpyrifos) were obtained from Sigma-Aldrich (St. Louis, MO). Whey protein isolate

(WPI) was donated by Agropure Dairy Cooperative (Le Sueur, MN). The enzymes and biopolymers, mucin (M2378), pepsin (P7000), porcine lipase (L3126), and porcine bile extract (B8631), used for digestion were obtained from Sigma-Aldrich (St. Louis, MO). A water purification system (Nanopure Infinity, Barnstaeas International, Dubuque, IA) was used to prepare the double distilled water used in this study. Only analytical grade chemicals, solvents, and reagents were utilized in the study.

2.2 Emulsion preparation

We produced the emulsions by mixing 10 wt% oil phase (corn oil) with 90 wt% water phase (1 wt% WPI in 5 mM phosphate buffer, pH 7.0). The "large" emulsions were formed by blending with a bio-homogenizer (M133/1281-0, Biospec Products, Inc., ESGC, Switzerland) for 2 min. The "small" emulsions were produced by circulating large emulsions three-times through a microfluidizer (M110Y, Microfluidics, Newton, MA) equipped with a 75 μm interaction chamber (F20Y) at 11,000 psi. The bulk oil samples were prepared by simply adding corn oil (same amount as in the emulsions) to the samples. All the samples were diluted to a final oil content of 8 wt% before use. All solutions were prepared using phosphate buffer (5 mM, pH 7) unless otherwise stated.

2.3 Preparation of model pesticide-treated agricultural produce

Pesticides were mixed with tomatoes to mimic a pesticide-treated agricultural produce. Fresh organic tomatoes were washed under running water for 1 min and wiped dry using tissue paper. The tomato was then cut into small cubes (around 10 × 10 mm) to facilitate tissue fragmentation during blending, which was carried using a commercial kitchen blender for 1 min. Afterward, the tomato puree produced was mixed with a pesticide solution containing a known pesticide concentration. Individual pesticide solutions were produced by weighing pesticide powders into acetonitrile to reach final concentrations of bendiocarb, parathion, and chlorpyrifos of 1.0, 1.0 and 5.0 mg/mL (10, 10, and 50 ppm), respectively. These concentrations were selected based

on the fact that they were 100-fold higher than the maximum residue (MRL) levels [19-21], which led to a pesticide concentration in the samples that was high enough to detect using HPLC after the whole digestion process.

2.4 Gastrointestinal tract model

The simulated gastrointestinal tract model used in this study was the same as the one used in our previous study[22]. Briefly, initial samples were produced by combining equal masses of pesticide-treated tomato with model food samples containing different lipid phase dimensions. These mixed samples were then sequentially passed through the mouth, stomach, and small intestine phases as described previously. The physicochemical and structural properties of samples were measured after each digestion step.

2.5 Lipid digestion profile

The lipid digestion profiles were measured using an automatic titrator (Metrohm, USA) to neutralize the free fatty acids generated during lipid hydrolysis. The free fatty acids released from the samples were calculated using the following equation:

$$\%FFA = 100 \times (\frac{V_{NaOH} \times m_{NaOH} \times M_{Lipid}}{W_{Lipid} \times 2})$$

Here V_{NaOH} is the NaOH volume (mL) consumed to neutralize the free fatty acids, m_{NaOH} is the normality of the NaOH solution used to carry out the titration (0.25 N), W_{Lipid} is the total weight of lipid initially present in the reaction vessel (0.15 g), and M_{Lipid} is the molecular weight of the oil phase (800 g/mol for corn oil).

2.6 Particle characterization

The particle size and charge were also determined using the methods described in our previous study[22]. Briefly, the particle size characteristics were measured by static light scattering (Mastersizer 2000), whereas the particle charge characteristics were measured by electrophoresis (Zetasizer Nano ZS). Both analytical instruments were purchased from Malvern Instruments (Malvern, Worcestershire, UK). Before analysis,

the initial, mouth, and small intestine samples were diluted with phosphate buffer (pH 7), while the stomach samples were diluted with acidified-water (pH 3) to achieve an appropriate laser intensity. Refractive indices of 1.47 and 1.33 were used for corn oil and water in the calculations, respectively [23]. The particle size characteristics of the samples are reported as surface-weighted mean diameters (d_{32}) and full particle size distributions (PSDs).

The microstructures of the samples were recorded using confocal fluorescence microscopy with a 40× objective lens (Nikon, Melville, NY). Nile Red solution (1mg/mL ethanol) was mixed with each sample at a ratio of 20:1 to dye the oil phase. An excitation and emission wavelength of 543 and 605 nm were used to observe the oil phase, respectively.

2.7 Pesticides bioaccessibility

Pesticide bioaccessibility was measured after the mixed samples had been passed through each state of the model gastrointestinal tract, as described in our previous study [14]. The pesticide concentration in the total digest (C_{Digest}), as well as in the mixed micelle phase ($C_{micelle}$) collected after centrifugation of the digest, were measured. The bioaccessibility was then estimated using the following equation:

$$Bioaccessibility\ (\%) = 100\% \times \frac{C_{Micelle}}{C_{Digest}}$$

2.8 Pesticide quantification

Initially, 5 mL aliquots of digest or mixed micelle phase were mixed with 2.5 mL dichloromethane, vigorously agitated for 1 min, and then separated by centrifugation at 4000 rpm for 5 mins. After this process, the majority of the hydrophobic pesticides moved into the upper organic solvent phase (supernatant). This upper layer was collected and placed into a separate tube and then the samples were extracted one more time. The combined supernatants were then dried under nitrogen in a low light environment. The residues produced were then re-dissolved in acetonitrile to the required concentration before being filtered through a 0.45 μm PTFE filter.

An Agilent HPLC system was used to separate and quantify the pesticides, which was comprised of a binary pump, an inline degassing unit, an auto-sampler, a temperature controller, and an UV detector. A reversed-phase column (Zorbax SB-C18, 250 mm x 4.6 mm id, 5 μm) was used to separate the pesticides using a mobile phase of acetonitrile:0.1% formic acid (70:30) at a flow ratio of 1 mL/min. An injection volume and temperature of 20 μL and 30 °C were used, respectively. The bendiocarb, parathion and chlorpyrifos were detected at wavelengths of 210, 275 and 288 nm, respectively. The signals were acquired and analyzed using the instrument software (Agilent ChemStation) and pesticide concentrations were calculated using standard curves.

2.9 Statistical analysis

SPSS software was used to perform statistical analysis of data obtained from at least three fresh samples. Results are reported as average values ± standard deviations (SD). A Duncan's test was used to determine the significant difference ($P < 0.05$) between samples.

3. Results and Discussions

3.1. Initial properties of emulsions

In this study, emulsions containing "large" (d_{32} = 10 μm) and "small" (d_{32} = 0.14 μm) oil droplets were used to assess the influence of lipid phase dimensions on bioaccessibility. Initially, both emulsions were monomodal with only a single broad peak in the PSD (**Figure 2a**). The ζ-potential values of the large and small emulsions were -66 and -42 mV, respectively, which are consistent with previous studies using a similar emulsifier [14]. This negative charge is due to the whey proteins that form an interfacial coating around the lipid droplets, since they are anionic at pH values that exceed their isoelectric point (pI = 5). The reason the magnitude of the surface potential was different for the large and small emulsions could be due to variations in the amount or organization of the adsorbed proteins. However, it may also be a result of the fact

that the ζ-potential is calculated from the electrophoretic mobility measurements using a model that assumes the particle size does not change [24]. A bulk oil sample was also prepared, but the particle characteristics of this system could not be assessed until it was blended with the other components.

3.2. Impact of GIT conditions on particle characteristics

Model food samples with different lipid phase dimensions (emulsions and bulk oil) were then mixed with pesticide-contaminated tomatoes. The particle characteristics of the resulting mixtures were measured after exposure to successive GIT stages. In this section, we only show the results for the tomato samples treated with bendiocarb because all of the other pesticide-treated samples showed similar behavior. Presumably, this is because the small amount of pesticide added to the tomato puree had little impact on particle properties.

Initial samples. Initially, model foods with different lipid phase dimensions were blended with pesticide-treated tomato puree. The resulting samples therefore contained mixtures of large fragments of plant tissue, as well as lipid droplets from the model foods. The mean particle diameters of the mixed samples depended on the initial dimensions of the lipid phase (**Figure 1**). The PSD measurements showed that the initial samples had some very large particles within them (presumably tomato tissue fragments), as well as some smaller particles (presumably lipid droplets) (**Figure 2b**). In our previous study, we measured the PSD of tomato samples alone (no oil), which showed that they contained only large particles, which supports this identification of the different particles in the system [25]. The mean particle diameter is calculated from the PSD, and so a population of small lipid droplets would lead to a smaller d_{32} value for the mixed system.

Interestingly, the PSD measurements indicated that there was a substantial increase in the size of the lipid droplets in the mixed samples containing the small emulsion compared to the original small emulsion (**Figure 2b**). Conversely, there was little

change in the dimensions of the lipid droplets within the mixed samples containing the large emulsion. This result was supported by confocal microscopy analysis, which showed that appreciable flocculation of the lipid droplets had occurred in the small emulsions after they were combined with the tomato puree (**Figure 3**). The origin of this effect may be the pH change that occurred when the original emulsion was mixed with the tomato puree. The pH in the emulsions went from neutral (pH 7) before mixing to acidic (pH 4) after mixing, which may have promoted flocculation of the protein-coated lipid droplets because of the reduction in their electric charge near their isoelectric point. Our previous study showed that when similar samples were adjusted back to pH 7, most of these flocs dissociated, indicating that flocculation was pH-driven and mainly reversible[14]. Nevertheless, we did observe a small amount of irreversible flocculation when the pH was adjusted back to 7 in the current study, which may have been due to the interactions of the lipid droplets with other constituents in the tomato puree. For instant, tomatoes contain biopolymers (like pectin) that may have promoted bridging or depletion flocculation[22], as well as mineral ions (like sodium or calcium) may have promoted electrostatic flocculation due to ion bridging, binding or screening effects[26, 27]. A large change in the dimensions of the individual lipid droplets in the mixed samples prepared using the large emulsion or bulk oil was not observed (**Figure 3**), which may have been because these large droplets could not move around as readily.

The ζ-potential measurements provided some insights into particle surface composition (**Figure 4**). The particles in all the mixed samples had a net negative charge, even though the pH of these samples (pH 4) was below protein isoelectric point (pH 5). This suggests that anionic biopolymers, such as pectin, from the tomato puree may have become attached to the protein-coated lipid droplets. Moreover, the samples prepared from the bulk oil had the strongest negative charge, which may have been because they did not contain any positively charged whey protein molecules. Instead, their charge was mainly a result of the anionic tomato fragments.

Mouth. An appreciable rise in particle dimensions occurred after samples were incubated under simulated mouth conditions, with the effect being most pronounced for mixed systems prepared from small emulsions (**Figure 1**). The PSD measurements suggested that this change was mainly due to a reduction in the fraction of small particles present in the mixed systems (**Figure 2c**), which is consistent with our previous study [25]. The confocal microscopy images suggest that there was a change in the characteristics of the flocs formed in the system after incubation in oral fluids (**Figure 3**). These changes in structural organization could be due to changes in solution pH, as well as due to the presence of mucin and mineral ions in the artificial saliva. The system increased from pH 4 to 7 after mixing the saliva, leading to a relatively large negative surface potential on the protein-coated droplets, thus reducing the susceptibility to bridging flocculation, as well as strengthening the electrostatic repulsion between the droplets. Even so, mucin molecules may still have promoted bridging or depletion flocculation, while mineral ions may still have promoted electrostatic flocculation.

The net particle was negative in all the samples after incubation in simulated saliva: -26, -34, and -46 mV for the bulk oil, large emulsions, and small emulsions, respectively (**Figure 4**). Compared to the initial samples, the absolute value of the negative charge decreased slightly for the bulk oil sample, but increased greatly for the large and small emulsions. The slight decrease observed in the bulk oil samples was probably caused by screening of the electrostatic interactions by mineral ions within the artificial saliva. On the contrary, the appreciable increase observed in the emulsion samples is probably because the protein-coated droplets have a strong negative potential in simulated oral conditions. Even so, after incubation under simulated mouth conditions, the charge intensity of the large and small emulsions was still lower than their original values (-66 and -42 mV at pH 7, respectively), which again indicated some electrostatic screening effects by mineral ions from the saliva [28].

Stomach. After passing through simulated stomach conditions, no appreciable change in the particle size was observed for the mixed samples prepared from bulk oil or large emulsions, but a slight decrease was observed for those prepared from small emulsions (**Figure 1**). The PSD measurements indicate that this change is due to a rise in the percentage of smaller particles present in the samples (**Figure 2d**), which is consistent with changes in floc structure seen in the mouth phase. Indeed, the microstructure images of the mixed samples containing small emulsions indicate that large tenuous flocs were present in the mouth, but somewhat smaller and more compact ones were present in the gastric fluids. The microstructure images also show that there were a number of large individual oil droplets present in the gastric fluids for the bulk oil and large emulsion samples, but that they were further apart than in the saliva fluids, which is due to dilution effects.

It should be noted that the particle dimensions determined by light scattering depend on the size, concentration, and refractive index of the various kinds of particle present in a mixed system. For this reason, they should be treated with some caution because both lipid droplets and plant tissue fragments, which may be present in different aggregation states, will make contributions to the light scattering pattern. Moreover, samples have to be diluted and stirred prior to light scattering analysis, which can cause changes in their structural organization. Confocal microscopy, therefore, is a more reliable method of observing structural changes in lipid phases in foods under gastrointestinal conditions [29].

The surface charge of all mixed samples was close to zero after incubation in the stomach phase. This effect has also been reported in previous studies on closely related systems [14], where it was attributed to a loss of negative charge on the carboxyl groups on tomato fragments at low pH values, as well as charge neutralization caused by the coating of cationic protein-coated lipid droplets with anionic biopolymers under gastric conditions [30].

Small Intestine. After passing through the simulated small intestine stage, the bulk oil and large emulsion samples exhibited a slight decrease in particle size, but the small emulsion samples showed a pronounced decrease (**Figures 1 and 2e)**. These changes are mainly due to hydrolysis of the triglycerides inside the lipid droplets. In the bulk oil and large emulsion samples, not all of the lipid droplets were fully digested, leaving some relatively large lipid-rich fragments (**Figure 3**). Conversely, all the droplets within the small emulsion appeared to have been completely hydrolyzed after 2 hours exposure to small intestine conditions. The influence of lipid phase dimensions on lipid hydrolysis were confirmed by the pH-stat measurements discussed later (**Section 3.3**).

All samples had a strong negative charge after being digested within the small intestine phase (**Figure 4**). This effect is the result of the presence of a mixture of anionic particles, such as mixed micelles, partially digested oil droplets, insoluble calcium salts, proteins, and plant tissue fragments, after digestion. The magnitude of the negative charge depended on the initial lipid phase dimensions in the mixed samples: small emulsions led to a higher negative charge than bulk oil or large emulsions. This effect is probably because the small emulsions were fully digested and so released more anionic fatty acids that contributed to the negative charge.

3.3. Lipid digestion profiles

Next, the impact of lipid phase dimensions on digestion was studied. The free fatty acids generated throughout the simulated small intestine phase were monitored by continuous neutralization of the system using an alkaline solution.

The lipid digestion rate and extent clearly depended on the initial lipid phase dimensions in the mixed samples: the smaller the lipid droplets, the faster the initial rate of digestion and the higher the final extent of digestion (**Figure 6**). In general, the rate of lipid digestion in emulsions is limited by the specific surface area of lipids exposed to lipase. A theoretical model was proposed by McClements and Li to

describe this phenomenon [31], which was later corrected by Gaucel and co-workers [32] to give:

$$\Phi(\mathrm{t}) = \phi_{max}(1 - (1 - \frac{Mkt}{d_0\rho})^{3})$$

The parameters represented in the equation are: $\Phi(\mathrm{t})$, the free fatty acids (FFAs) release at time t, $\phi_{\max}$, the maximum amount of FFAs released, k, the digestion rate constant, d_0, the initial surface-weighted mean droplet diameter (d_{32}), M, the lipid molecular weight, and ρ, the lipid density. This equation assumes that the diameter of the individual lipid droplets steadily decreases during lipid hydrolysis as the triacylglycerols are broken down into FFAs and monoglycerides, which then leave the droplet surfaces [31]. It should be noted that the droplet size used in this equation should be the one at the start of the small intestine phase, rather than the initial one. The above model therefore indicates that the smaller the initial dimensions of the lipid droplets in the small intestine, the faster the initial rate of lipid digestion. The faster rate of the mixed sample containing the small emulsion can therefore be attributed to the fact that it contained smaller individual droplets when it entered the small intestine phase. Indeed, the confocal microscopy images show that the individual lipid droplets are much smaller in this system when the samples leave the stomach phase (**Figure 4**).

The final amount of lipids produced was also dependent on the initial lipid phase dimensions. The total free fatty acids released were 104%, 88%, and 75% for small emulsions, large emulsions and bulk oil, respectively (**Figure 6b**). Presumably, this effect was due to slower hydrolysis of the triglycerides in the samples containing large lipid droplets (lower surface areas) [31]. In other words, the lipid phase in these samples has not been completely digested after 2 hours. Under *in vivo* conditions, these undigested lipids may pass into the colon where they may be metabolized by the gut microbiome. High levels of undigested fats inside the colon may promote certain

health problems, which should be considered when formulating foods. It should be noted, however, that most food emulsions are likely to be fully digested within the human GIT, albeit at a slower rate for larger droplets.

3.3. Pesticides Bioaccessibility

Next, the impact of initial lipid phase dimensions on pesticide bioaccessibility was studied. Bendiocarb, parathion, and chlorpyrifos were selected due to their significantly different polarities. As initially hypothesized, the bioaccessibility of the pesticides depended on both lipid phase dimensions and pesticide polarity.

The most polar pesticide, bendiocarb (Log P = 1.7), had a high bioaccessibility (around 100%) that did not depend on the dimensions of the lipid phase in the model food co-ingested with it (**Figure 6a**). This may be because the concentration of bendiocarb used in this study (100 mg/L) was much lower than its water-solubility (260 mg/L at 25 ^{o}C) (chemspider.com). For this reason, the bendiocarb was almost completely located within the water phase and so its bioaccessibility did not depend on the dimensions of the lipid phase. Conversely, the bioaccessibility of the more hydrophobic pesticides (parathion, Log P = 3.8; chlorpyrifos, Log P = 5.3) were considerably lower than that of bendiocarb and depended on lipid phase dimensions (**Figures 6b and 6c**). This is because the levels of parathion and chlorpyrifos (500 and 100 mg/L) used in this study were considerably higher than their water solubilities (11 mg/L and 1.1m g/L at 25 ^{o}C, respectively) (chemspider.com). As a result, most of these pesticides were located within the oil phase of the mixed systems. For the bulk oil and large emulsions, a fraction of lipid phase was not digested after 2 hours of hydrolysis. For this reason, some of the pesticides remained inside the non-digested lipid phase. Moreover, there would have been less FFAs and monoglycerides released that could assemble into mixed micelles capable of solubilizing the hydrophobic pesticides. Therefore, the maximum amount of pesticides that could be solubilized would be reduced.

The influence of pesticide polarity and droplet size on the bioaccessibility of the pesticides was highlighted by plotting the bioaccessibility ratio (BR) *versus* the droplet-size ratio (DR) (**Figure 7**). Here, BR is the bioaccessibility of the pesticide for a particular sample divided by the bioaccessibility of the same pesticide in bulk oil. Similarly, DR is the diameter of the oil droplets in an initial emulsion sample divided by the diameter of the oil droplets in the initial bulk oil sample. The slope of the linear regression equation was -0.57 and -0.33 for samples containing parathion and chlorpyrifos, respectively, indicating a significant decrease in bioaccessibility with increasing droplet size. On the other hand, the slope of the linear regression equation was close to zero (0.04) for the bendiocarb samples, indicating that its bioaccessibility did not depend on droplet size. From Figure 7, the impact of droplet size of lipids on the bioaccessibility of different pesticides is clear: decreasing the droplet size significantly increases the bioaccessibility of hydrophobic pesticides, but has little impact on that of hydrophilic pesticides.

4. Conclusions

Our results show that pesticide bioaccessibility is highly dependent on pesticide polarity and the lipid phase dimensions of foods consumed with them. The most polar pesticide, bendiocarb (Log P = 1.7), had a high bioaccessibility (>95%) that was independent of lipid phase dimensions. We propose that this effect is because this polar pesticide is mainly located within the water phase of the gastrointestinal fluids. Conversely, the more non-polar pesticides, parathion (Log P = 3.4) and chlorpyrifos (Log P = 5.3), had much lower bioaccessibilities that depended on lipid phase dimensions. In particular, the bioaccessibility decreased with increasing lipid droplet size because less of the lipids were fully digested. These findings provide some useful insights into the potential impact of food matrix effects on the absorption of pesticides from agricultural products that may be consumed with fatty foods, such as fruits and vegetables.

5. Acknowledgements

This material is based upon work supported by the Cooperative State Research, Extension, Education Service, United State Department of Agriculture, Massachusetts Agricultural Experiment Station (Project No. 831) and by the United States Department of Agriculture, NRI Grants **(2016-08782).**

6. References

1. F. P. Carvalho, Agriculture, pesticides, food security and food safety, *Environmental science & policy*, 2006, **9**, 685-692.

2. D. Goulson, An overview of the environmental risks posed by neonicotinoid insecticides, *Journal of Applied Ecology*, 2013, **50**, 977-987.

3. L. Nasreddine and D. Parent-Massin, Food contamination by metals and pesticides in the European Union. Should we worry?, *Toxicology letters*, 2002, **127**, 29-41.

4. C. E. Handford, C. T. Elliott and K. Campbell, A review of the global pesticide legislation and the scale of challenge in reaching the global harmonization of food safety standards, *Integrated environmental assessment and management*, 2015, **11**, 525-536.

5. A. Priyadarshi, S. A. Khuder, E. A. Schaub and S. Shrivastava, A meta-analysis of Parkinson's disease and exposure to pesticides.*Journal*, 2000.

6. I. Baldi, P. Lebailly, B. Mohammed-Brahim, L. Letenneur, J.-F. Dartigues and P. Brochard, Neurodegenerative diseases and exposure to pesticides in the elderly, *American journal of epidemiology*, 2003, **157**, 409-414.

7. J. Dich, S. H. Zahm, A. Hanberg and H.-O. Adami, Pesticides and cancer, *Cancer Causes & Control*, 1997, **8**, 420-443.

8. M. C. R. Alavanja, J. A. Hoppin and F. Kamel, Health effects of chronic pesticide exposure: cancer and neurotoxicity, *Annu. Rev. Public Health*, 2004, **25**, 155-197.

9. K.-H. Kim, E. Kabir and S. A. Jahan, Exposure to pesticides and the associated human health effects, *Science of the Total Environment*, 2017, **575**, 525-535.

10. A. Sabarwal, K. Kumar and R. P. Singh, Hazardous effects of chemical pesticides on human health–Cancer and other associated disorders, *Environmental toxicology and pharmacology*, 2018, **63**, 103-114.

11. Á. G. P. Rodríguez, M. I. R. López, T. Á. D. Casillas, J. A. A. León, O. Mahjoub and A. K. Prusty, Monitoring of organochlorine pesticides in blood of women with uterine cervix cancer, *Environmental Pollution*, 2017, **220**, 853-862.

12. N. S. Singh, R. Sharma, T. Parween and P. Patanjali, in *Modern Age Environmental Problems and their Remediation*, Springer, 2018, pp. 49-68.

13. K. Knauer, N. Homazava, M. Junghans and I. Werner, The influence of particles on bioavailability and toxicity of pesticides in surface water, *Integrated environmental assessment and management*, 2017, **13**, 585-600.

14. R. Zhang, W. Wu, Z. Zhang, Y. Park, L. He, B. Xing and D. J. McClements, Effect of the composition and structure of excipient emulsion on the bioaccessibility of pesticide residue in agricultural products, *Journal of agricultural and food chemistry*, 2017, **65**, 9128-9138.

15. R. Zhang, W. Wu, Z. Zhang, S. Lv, B. Xing and D. J. McClements, Impact of Food Emulsions on the Bioaccessibility of Hydrophobic Pesticide Residues in Co-ingested Natural Products: Influence of Emulsifier and Dietary Fiber Type, *Journal of agricultural and food chemistry*, 2019.

16. R. Zhang and D. J. McClements, Enhancing nutraceutical bioavailability by controlling the composition and structure of gastrointestinal contents: Emulsion-based delivery and excipient systems, *Food structure*, 2016, **10**, 21-36.

17. R. Zhang, Z. Zhang, L. Zou, H. Xiao, G. Zhang, E. A. Decker and D. J. McClements, Enhancement of carotenoid bioaccessibility from carrots using excipient emulsions: influence of particle size of digestible lipid droplets, *Food & function*, 2016,

7, 93-103.

18. L. Zou, W. Liu, C. Liu, H. Xiao and D. J. McClements, Utilizing food matrix effects to enhance nutraceutical bioavailability: increase of curcumin bioaccessibility using excipient emulsions, *Journal of agricultural and food chemistry*, 2015, **63**, 2052-2062.

19. P. Aysal, K. Gözek, N. Artık and A. S. Tuncbilek, 14 C-Chlorpyrifos Residues in Tomatoes and Tomato Products, *Bulletin of environmental contamination and toxicology*, 1999, **62**, 377-382.

20. Z. Ghoraba, B. Aibaghi and A. Soleymanpour, Ultrasound-assisted dispersive liquid-liquid microextraction followed by ion mobility spectrometry for the simultaneous determination of bendiocarb and azinphos-ethyl in water, soil, food and beverage samples, *Ecotoxicology and environmental safety*, 2018, **165**, 459-466.

21. L. Zhang, Z. Wang, Y. Wen, J. Shi and J. Wang, Simultaneous detection of parathion and imidacloprid using broad-specificity polyclonal antibody in enzyme-linked immunosorbent assay, *Analytical Methods*, 2015, **7**, 205-210.

22. R. Zhang, Z. Zhang, H. Zhang, E. A. Decker and D. J. McClements, Influence of emulsifier type on gastrointestinal fate of oil-in-water emulsions containing anionic dietary fiber (pectin), *Food Hydrocolloids*, 2015, **45**, 175-185.

23. R. Zhang, Z. Zhang, H. Zhang, E. A. Decker and D. J. McClements, Influence of lipid type on gastrointestinal fate of oil-in-water emulsions: In vitro digestion study, *Food Research International*, 2015, **75**, 71-78.

24. D. J. McClements, *Food Emulsions: Principles, Practice and Techniques*, CRC Press, Boca Raton, FL, 2015.

25. R. Zhang, Z. Zhang, R. Li, Y. Tan, S. Lv and D. J. McClements, Impact of Pesticide Type and Emulsion Fat Content on the Bioaccessibility of Pesticides in Natural Products, *Molecules*, 2020, **25**, 1466.

26. R. Chanamai and D. McClements, Comparison of gum arabic, modified starch,

and whey protein isolate as emulsifiers: influence of pH, CaCl2 and temperature, *Journal of food science*, 2002, **67**, 120-125.

27. A. Kulmyrzaev, C. Bryant and D. J. McClements, Influence of sucrose on the thermal denaturation, gelation, and emulsion stabilization of whey proteins, *Journal of Agricultural and Food Chemistry*, 2000, **48**, 1593-1597.

28. A. Sarkar, K. K. T. Goh and H. Singh, Colloidal stability and interactions of milk-protein-stabilized emulsions in an artificial saliva, *Food Hydrocolloids*, 2009, **23**, 1270-1278.

29. C. Chung, B. Degner and D. J. McClements, Rheology and microstructure of bimodal particulate dispersions: Model for foods containing fat droplets and starch granules, *Food Research International*, 2012, **48**, 641-649.

30. Z. Zhang, R. Zhang, L. Zou and D. J. McClements, Protein encapsulation in alginate hydrogel beads: Effect of pH on microgel stability, protein retention and protein release, *Food Hydrocolloids*, 2016, **58**, 308-315.

31. Y. Li and D. J. McClements, New mathematical model for interpreting pH-stat digestion profiles: Impact of lipid droplet characteristics on in vitro digestibility, *Journal of agricultural and food chemistry*, 2010, **58**, 8085-8092.

32. S. Gaucel, I. C. Trelea and S. Le Feunteun, Comment on New Mathematical Model for Interpreting pH-Stat Digestion Profiles: Impact of Lipid Droplet Characteristics on in Vitro Digestibility, *Journal of Agricultural and Food Chemistry*, 2015, **63**, 10352-10353.

Figure 1. The surface-weighted mean particle diameter (d_{32}) of samples as they passing through the simulated gastrointestinal tract. Samples designated with different capital letters (A, B, C) were significantly different (Duncan, $p < 0.05$) when compared between different GIT conditions (same particle size). Samples designated with different lower case letters (a, b, c) were significantly different (Duncan, $p < 0.05$) when compared between different lipid phase dimensions (same GIT condition).

Figure. 2. Particle size distribution of samples with different lipid phase dimensions as they exposing to simulated GIT conditions.

Figure 3. Microstructure of original emulsions and samples with different lipid phase dimensions as they incubated at different GIT conditions.

Figure 4. The electrical characteristics (ζ-potentials) of samples containing different lipid phase dimensions. Samples designated with different capital letters (A, B, C) were significantly different (Duncan, $p < 0.05$) when compared between different GIT conditions (same particle size). Samples designated with different lower case letters (a, b, c) were significantly different (Duncan, $p < 0.05$) when compared between different particle size (same GIT condition).

Figure 5. The fatty acids released profile of samples with different lipid phase dimensions.

Figure 6. Impact of the lipid phase dimensions on the bioaccessibility of pesticides with different Log P value: (a) Bendiocarb (log P 1.7), (b) Parathion (log P 3.8) and (c) Chlorpyrifos (Log P 5.3). Samples designated with different capital letters (A, B, C, D) were significantly different (Duncan, $p < 0.05$) when compared between different lipid phase dimensions.

Figure 7. Plot of the bioaccessibility ratio of pesticides with different Log P value *versus* droplet-size ratio of lipids co-consumed. The best-fit linear regression lines were showed for each pesticide.

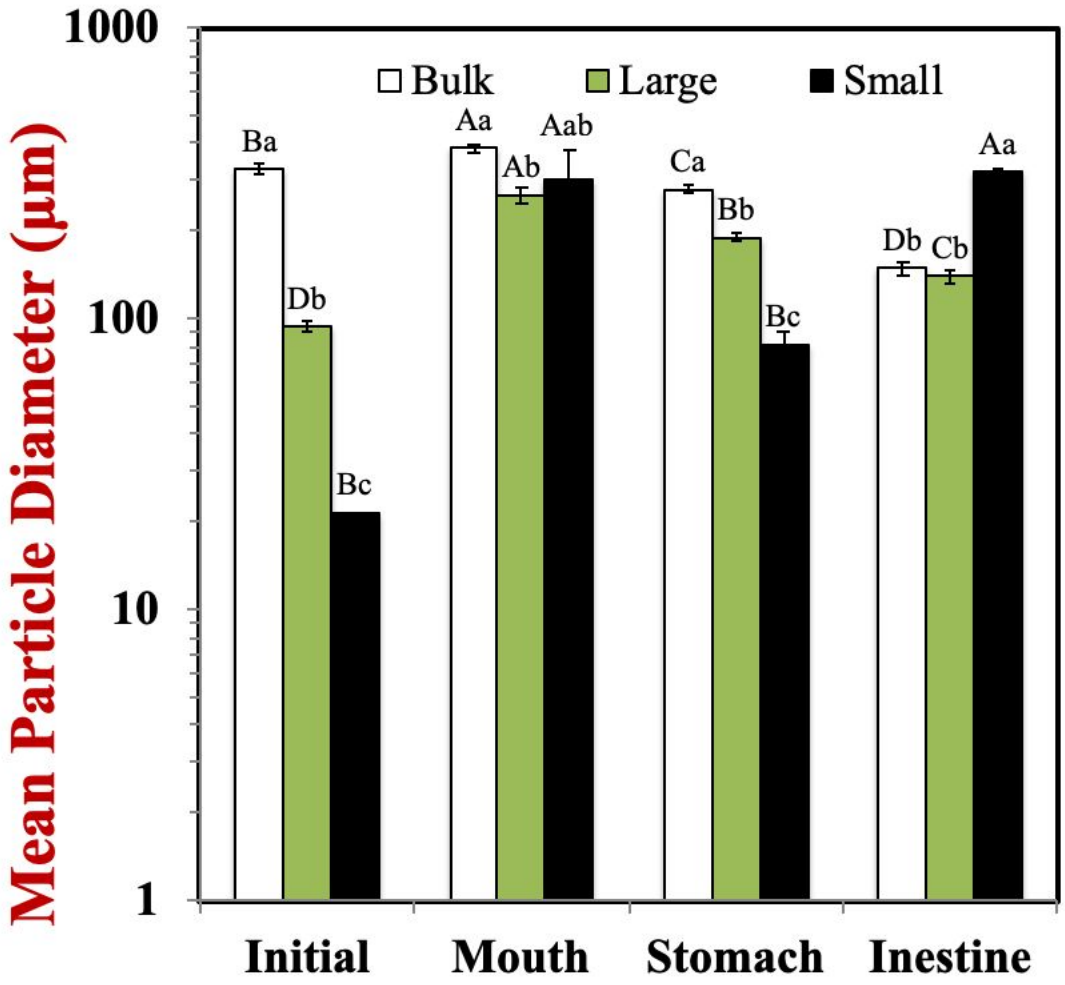
1000
100
10
1
Mean Particle Diameter (μm)
Bulk
Large
Small
Ba
Db
Bc
Aa
Ab
Aab
Ca
Bb
Bc
Db
Cb
Aa
Initial
Mouth
Stomach
Inestine

Fig. 1

37

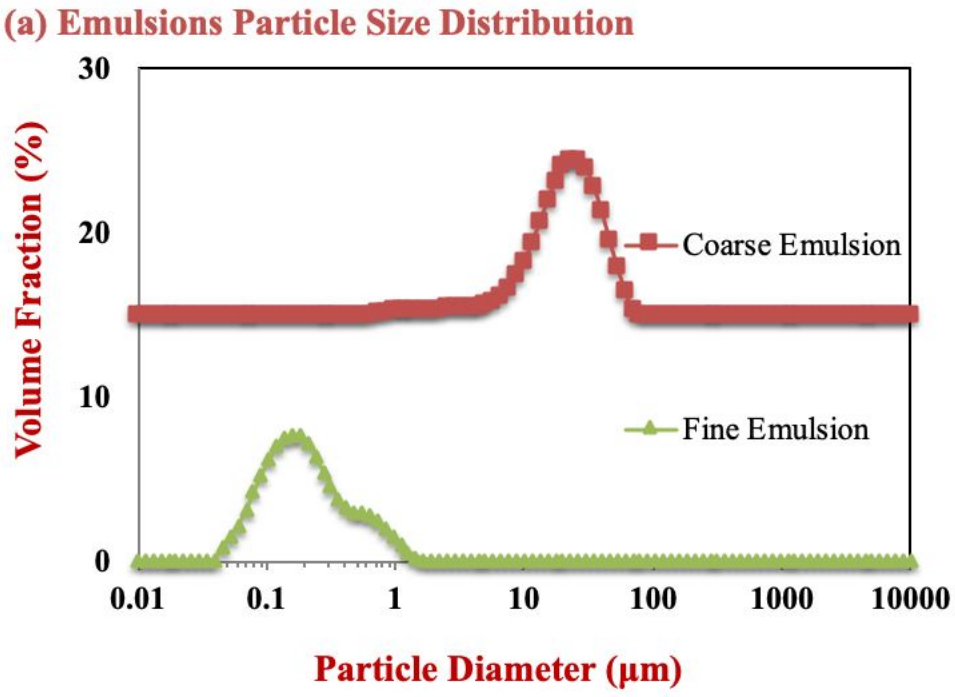
(a) Emulsions Particle Size Distribution
Volume Fraction (%)
30
20
10
0
Coarse Emulsion
Fine Emulsion
0.01
0.1
1
10
100
1000
10000
Particle Diameter (μm)

38

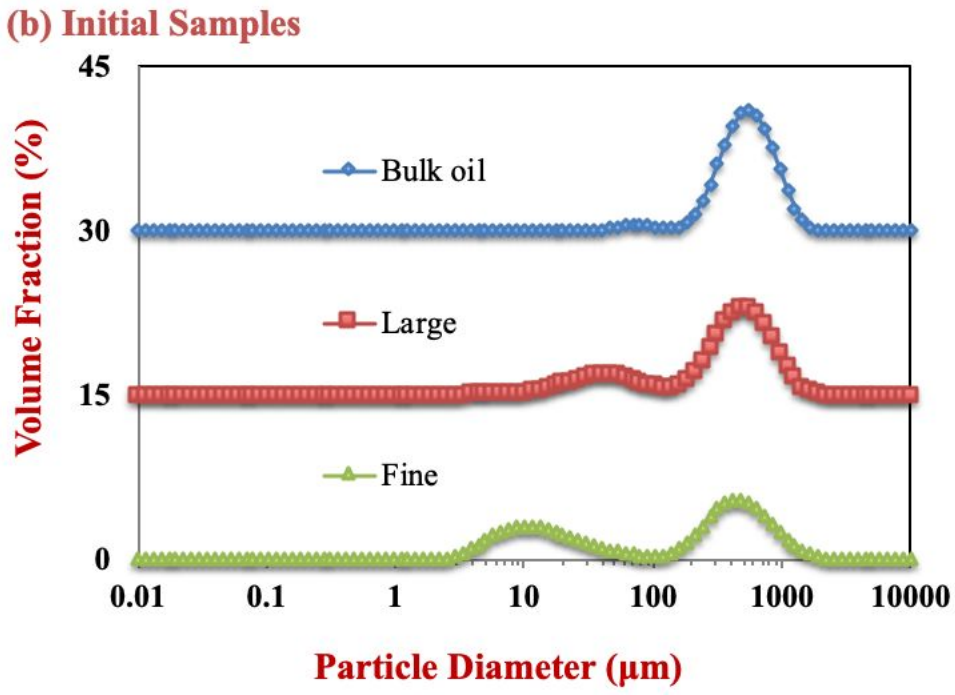
(b) Initial Samples
Volume Fraction (%)
45
30
15
0
Bulk oil
Large
Fine
0.01
0.1
1
10
100
1000
10000
Particle Diameter (μm)

39

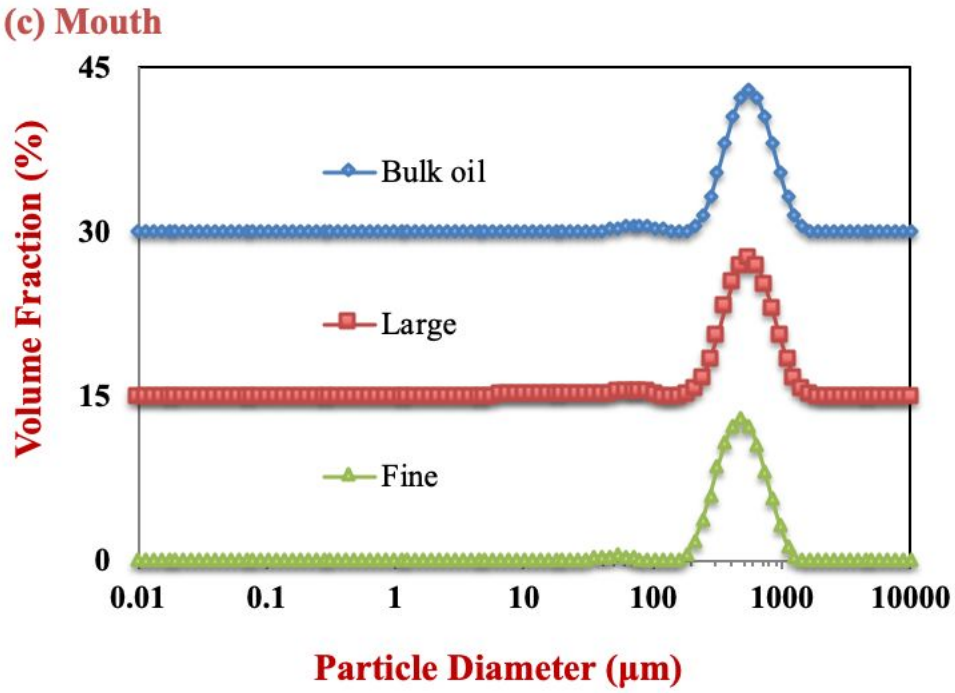
(c) Mouth
45
30
15
0
Volume Fraction (%)
Bulk oil
Large
Fine
0.01
0.1
1
10
100
1000
10000
Particle Diameter (μm)

40

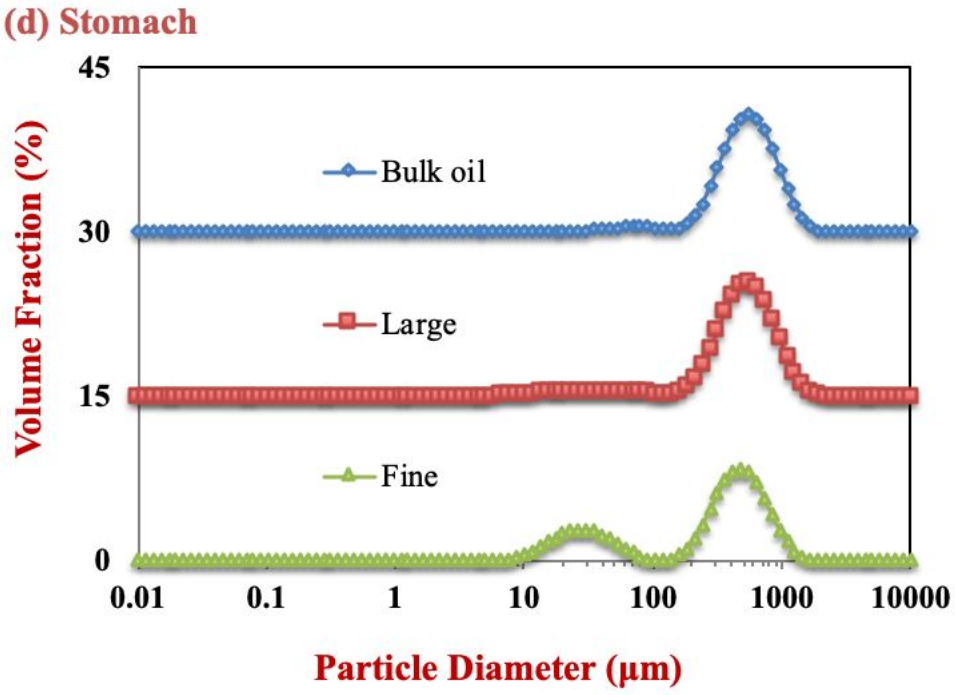
(d) Stomach
45
30
15
0
Volume Fraction (%)
Bulk oil
Large
Fine
0.01
0.1
1
10
100
1000
10000
Particle Diameter (μm)

41

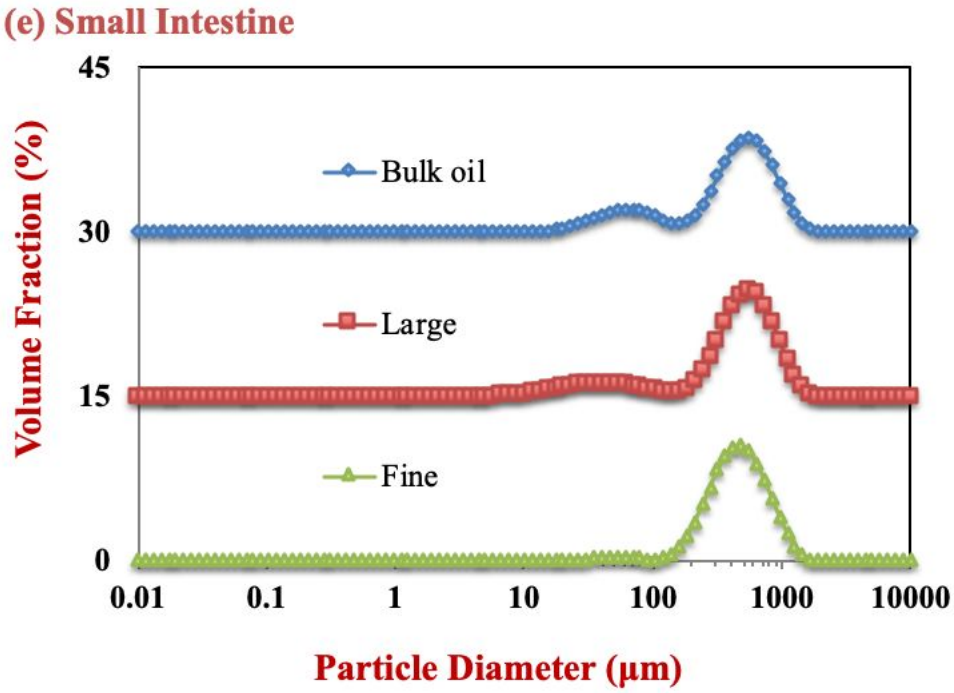
(e) Small Intestine
45
30
15
0
Volume Fraction (%)
Bulk oil
Large
Fine
0.01
0.1
1
10
100
1000
10000
Particle Diameter (μm)

Fig. 2

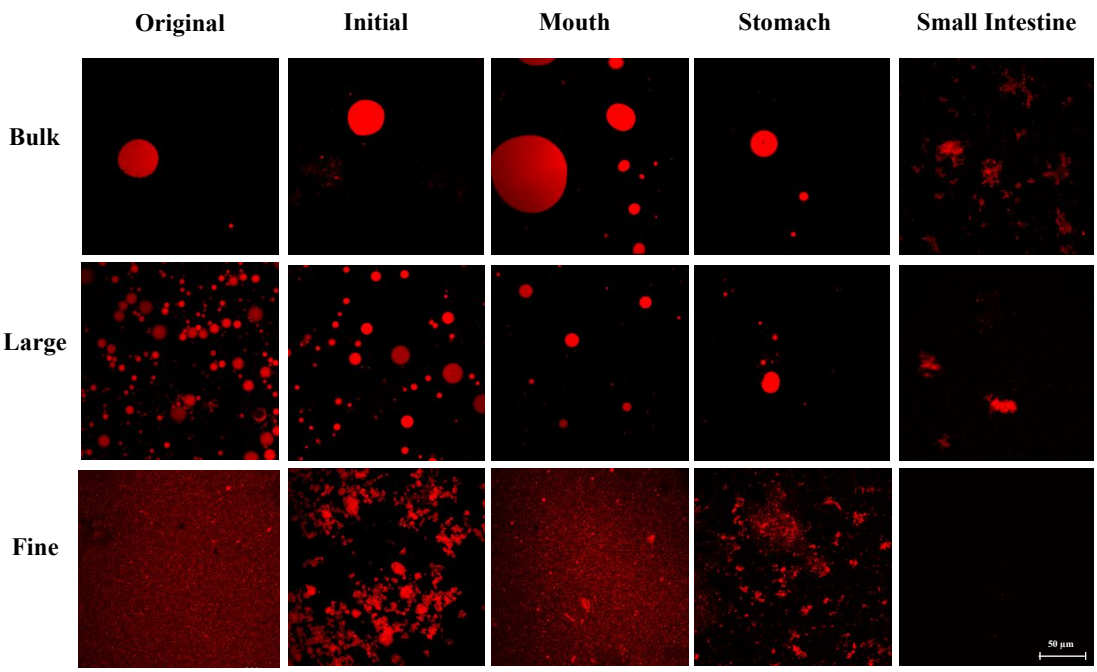
Original
Initial
Mouth
Stomach
Small Intestine
Bulk
Large
Fine
50 μm

Fig. 3

49

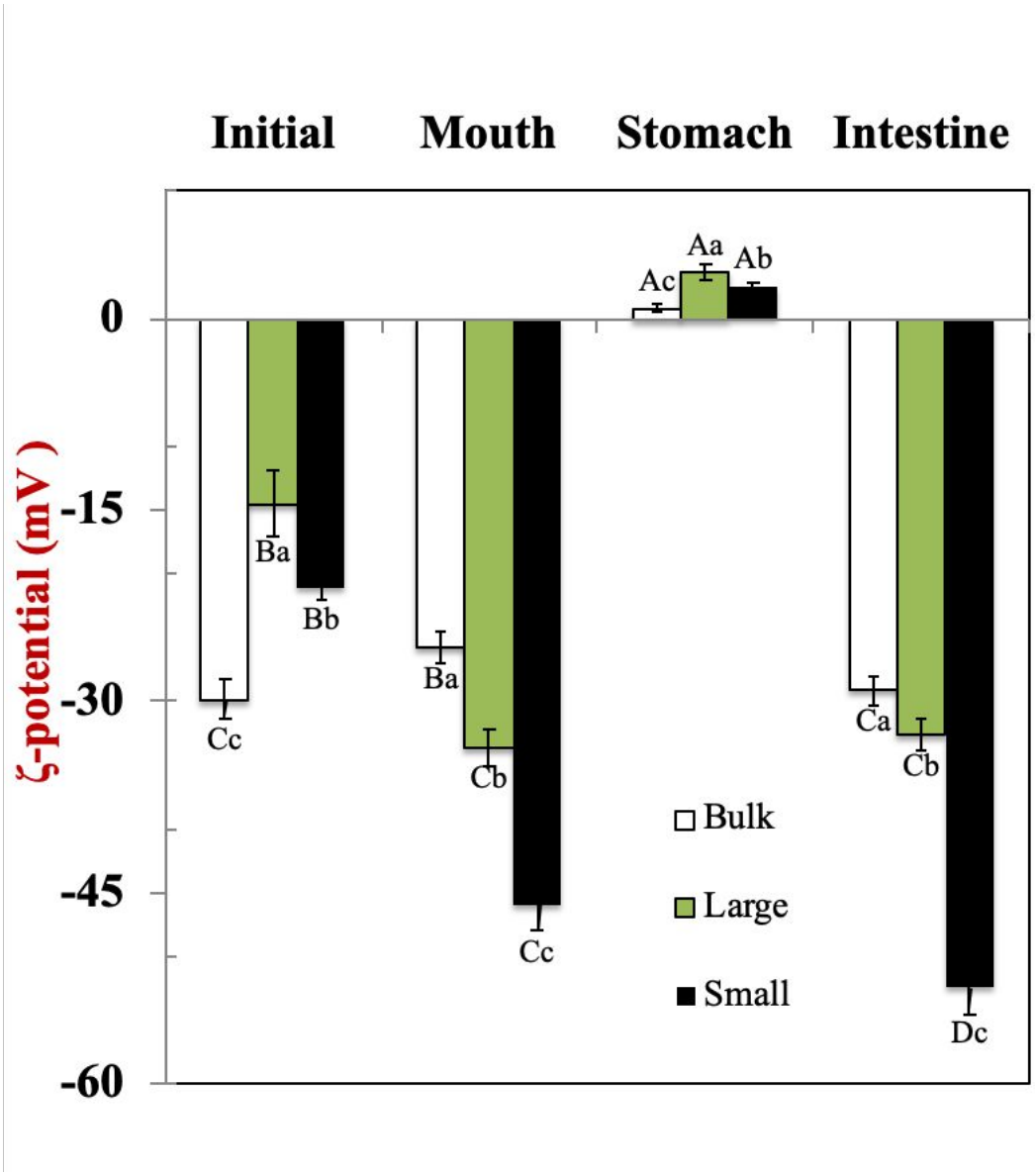

50

51

52 Fig. 4

53

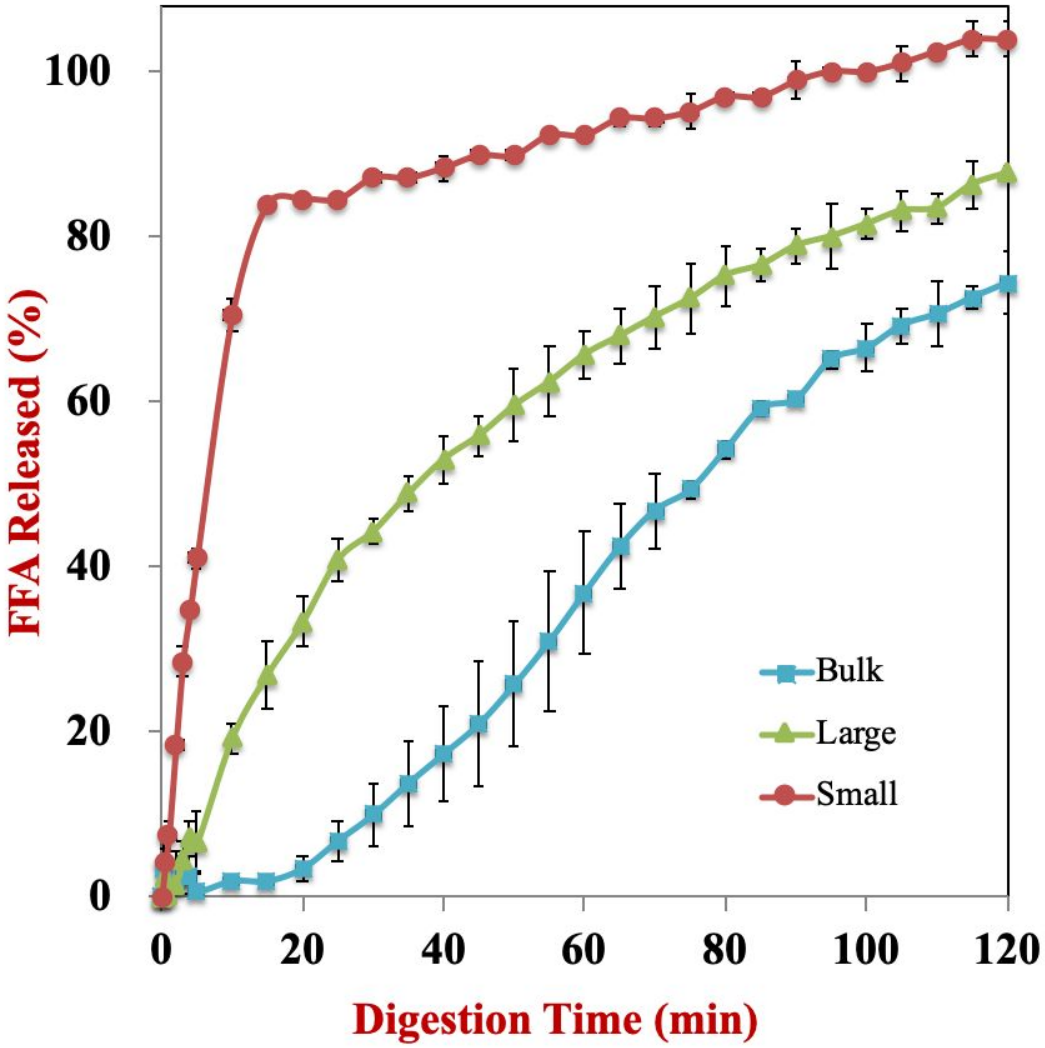
100
80
60
40
20
0
FFA Released (%)
0
20
40
60
80
100
120
Digestion Time (min)
Bulk
Large
Small

Fig. 5

57

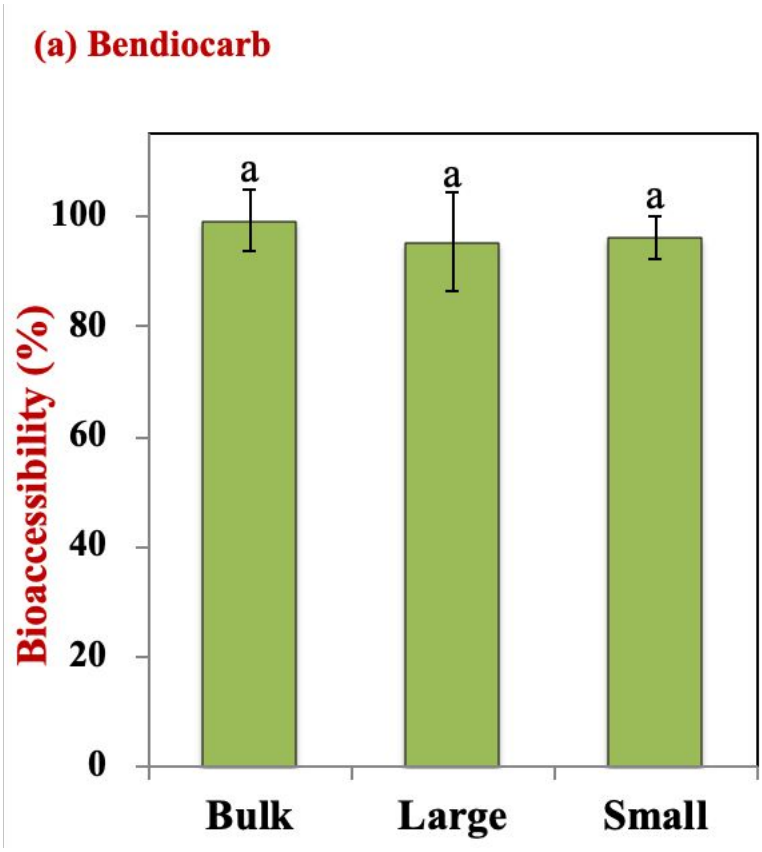
(a) Bendiocarb
Bioaccessibility (%)
0
20
40
60
80
100
a
a
a
Bulk
Large
Small

58

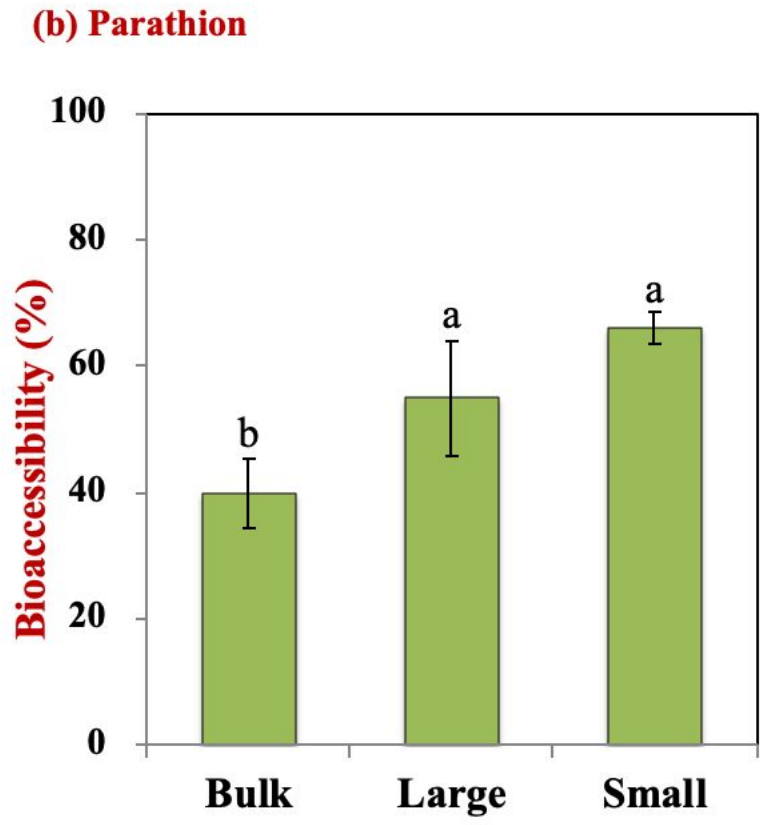
(b) Parathion
Bioaccessibility (%)
0
20
40
60
80
100
b
a
a
Bulk
Large
Small

59

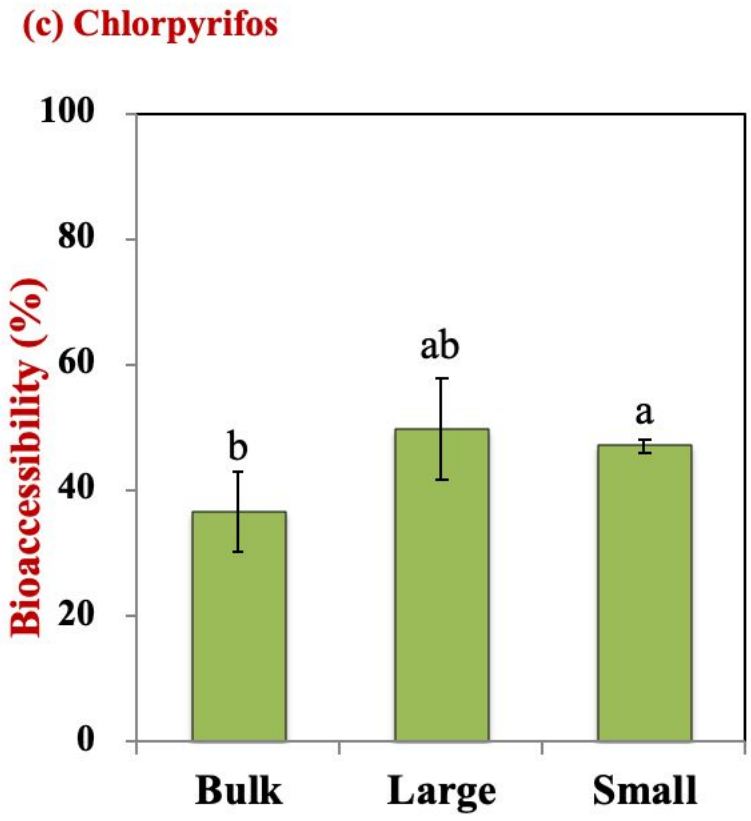
(c) Chlorpyrifos
Bioaccessibility (%)
100
80
60
40
20
0
b
ab
a
Bulk
Large
Small

Fig. 6

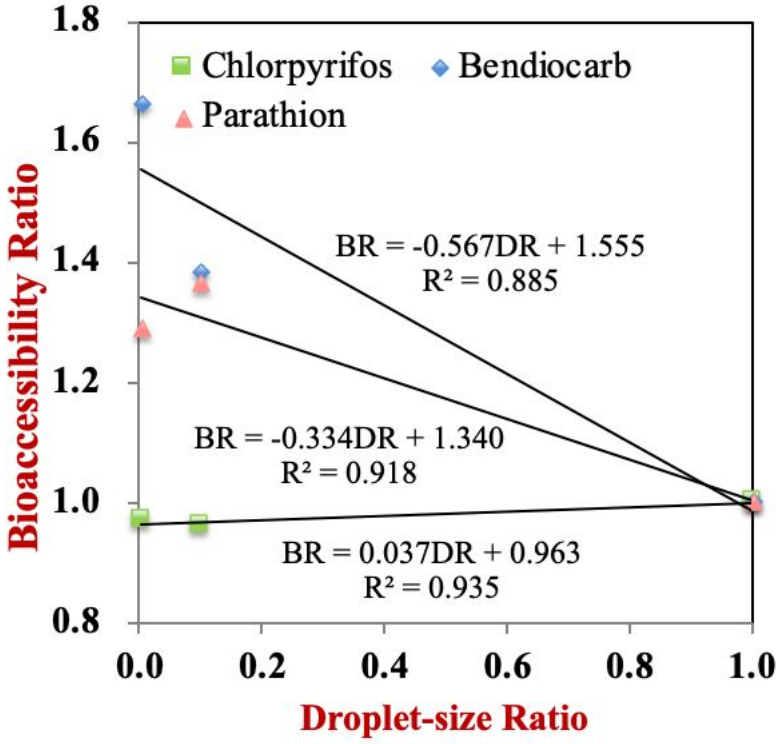
Chlorpyrifos
Bendiocarb
Parathion
BR = -0.567DR + 1.555
R² = 0.885
BR = -0.334DR + 1.340
R² = 0.918
BR = 0.037DR + 0.963
R² = 0.935
Bioaccessibility Ratio
Droplet-size Ratio
1.8
1.6
1.4
1.2
1.0
0.8
0.0
0.2
0.4
0.6
0.8
1.0

Fig.7